

Received November 10, 2016, accepted November 28, 2016, date of publication December 5, 2016, date of current version January 4, 2017.

Digital Object Identifier 10.1109/ACCESS.2016.2635718

Propagation Modeling in Large-Scale Cooperative Multi-Hop Ad Hoc Networks

MUHAMMAD AHSEN¹, SYED ALI HASSAN¹, (Member, IEEE), AND DUSHANTHA NALIN K. JAYAKODY², (Member, IEEE)

¹School of Electrical Engineering and Computer Science, National University of Sciences and Technology, Islamabad 44000, Pakistan

²Department of Software Engineering, Institute of Cybematics, National Research Tomsk Polytechnic University, 634050 Tomsk, Russia

Corresponding author: S. A. Hassan (ali.hassan@seecs.edu.pk)

This work was supported in part by the National ICT Research and Development Fund, Pakistan, in part by the Russian Federal Budget Funds for research work (Fundamental Research, Applied Research and Experimental Development) performed in accordance with the Russian Government Resolutions No. 2014/226 of 2016 under Grant 3942, and in part by the Ministry of Education and Science of the Russian Federation under Grant 02.G25.31.0190 dated 04.27.2016 and performed in accordance with Russian Government Resolutions No. 218 of 09.04.2010.

ABSTRACT In this paper, a strip-shaped multi-hop ad hoc network is analyzed using a spatial Poisson point process (PPP) and stochastic geometry. The decode-and-forward protocol is considered for transmission over the multi-hop network where cooperative communications is employed at each hop. An analytical expression for the probability density function of the received power at an arbitrary node is derived, given a set of nodes transmits in the previous hop, which is further used to characterize the coverage performance of the network. The received power at a node becomes a doubly stochastic process owing to random path loss and a Rayleigh fading channel. The notions of one-hop success probability and coverage range are analyzed for various network parameters. An algorithm for conserving energy is also proposed by considering PPP thinning and its performance in terms of the fraction of energy saved is quantified. It is shown that the proposed algorithm is more energy efficient as compared with an independent thinning algorithm.

INDEX TERMS Cooperative systems, fading channel, Poisson process, energy conservation.

I. INTRODUCTION

Future wireless networks pose critical challenges in terms of reliability and seamless coverage. Whereas future networks will be an amalgamation of sophisticated techniques under the umbrella of fifth generation (5G), an integral part of 5G communications will largely be composed of Internet of Things (IoT). Sensor and ad hoc networks constitute a major portion of IoT and communications between various entities of these networks plays a vital role for their successful operation. Cooperative transmission (CT) is one of the relaying techniques for wireless sensor and ad hoc networks used primarily to enhance the reliability of the received signals. The nodes cooperate to form a virtual antenna array and transmit the same signal towards the nodes of the next level or hop, thereby providing spatial diversity gain [1]. A CT multi-hop mechanism provides an efficient method for reaching a distant destination as the transmit powers of the nodes can be reduced without compromising the reliability [2].

Opportunistic Large Array (OLA) is a form of physical layer CT [3], where multiple nodes in a hop transmit the same

message, without any coordination among each other and without any addressing scheme. A promising characteristic of this technique is that it does not require any prior information of the number of cooperating nodes or their locations, which makes it scalable and suitable for transmission without any cluster head. In an OLA transmission, a source node broadcasts its message and all nodes in the vicinity that can decode this message, become part of level 1, which are known as decode-and-forward (DF) nodes. In the next time slot, these DF nodes transmit the same message concurrently in the forward direction using cooperation and the process continues until the data is reached at the destination or broadcasted to the entire network. However, the modeling of signal transmission over this multi-hop network is not very straightforward and the foremost model was proposed in [4].

The proposed model for a strip-shaped OLA network in [4] assumes infinite number of nodes transmitting constant power per unit area, which guaranteed infinite signal propagation over the network. This assumption of *continuum* of nodes confined its application to networks with very high

node density. However, it was shown in [5] that a finite node density cannot lead to an infinite broadcast and that the path loss exponent plays a major role in controlling the broadcast region. Hassan and Ingram [6] studied the OLA line network with finite node density and modeled the node locations with Bernoulli point process. This model is then extended in [7] to a strip-shaped network with deterministic hop boundaries. Specifically, the authors model an ad hoc network where the number of nodes in each hop is known a priori. Moreover, fixed hop boundaries were assumed and a Markov chain model was derived to study the characteristics of multi-hop transmissions over the network. We extend the model in [8] with random number of nodes per hop and fixed hop boundaries.

In this paper, we study the coverage of a more general setup, where the number of nodes per hop as well as hop boundaries are kept random. The transmission model resembles a typical OLA, where the transmission of the signal from a source to a distant destination forms irregular levels or hops with random number of nodes in each hop. We derive the coverage probability of this network using the distribution of the received power at a node, which is subject to channel impairments that include independent Rayleigh fading and path loss.

Our stochastic model is based on the theory of Poisson point process (PPP) [9], where the nodes in each hop are independent and distributed according to a Poisson random variable (RV). The analytical tractability of the PPP model makes it a suitable candidate to analyze the random number of nodes in each hop; unlike fixed number of nodes, which can be generally modeled using Markov chains [10]. Once modeled, the void probability of PPP is used to compute various network performance metrics such as m -hop success probability, coverage range (CR) and required node density to achieve a particular CR under a quality of service (QoS) constraint.

The proposed stochastic model helps in determining the CR of a pure OLA network given the node density of the network for various hop distances. It provides useful insights in designing a network in terms of one-hop success probability, m -hop success probability and fraction of energy saved (FES). Its applications include, but not limited to, smart grid communication system or fault recognition system for transmission lines, and structural health monitoring system for the overhead bridges and tunnels [11]. The model and its findings can also be used to set up an inter-vehicular communication system on the motorways [12] or a vehicular ad hoc network (VANET) to monitor highway activity by distributing the nodes along the highway.

The geometric complexity of the system increases with random node locations and irregular hop boundaries, making path loss a random process. The path loss is dependent upon the Euclidean distance between the nodes, which when combined with fading provides the notion of signal-to-noise ratio (SNR) for a single link. In CT, multiple single-input single-output (SISO) links are averaged over a PPP to analyze

virtual multiple-input single-output (MISO) links. Our main contributions in this paper are the followings.

- Derivation of the distribution of the Euclidean distance between a pair of nodes distributed randomly in adjacent overlapping levels without any hypothetical boundary in between them.
- It is shown with the help of some statistical approaches such as the moment matching method that the distribution of the distance raised to a positive power can be well approximated by a Weibull distribution.
- We derive the distribution of the received power for a virtual MISO link, which is the random sum over a PPP of the ratio of an exponential random variable (RV) and a Weibull RV.
- We derive the coverage range of a 2-dimensional (2D) strip-shaped multiple hop OLA network.
- We devise a thinning of PPP to conserve energy for the finite node density OLA networks with random node placements by allowing only a subset of nodes to transmit and quantify its performance.

An outline of the rest of the paper is as follows. Section II describes the system model for the strip-shaped OLA network under consideration. In Section III, the distance distribution between a pair of nodes is derived. Section IV characterizes the coverage behavior of the MISO links in terms of the coverage probability and one-hop success probability. Section V discusses the thinning algorithm and proves that the distribution and intensity of the new process obtained after thinning remains the same. Section VI validates our analytical model and presents some useful results pertaining to system performance metrics followed by the conclusion and future directions in Section VII.

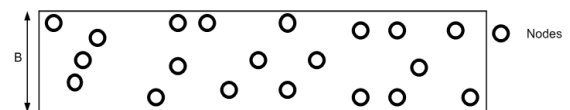


FIGURE 1. A 2D strip-shaped network with finite node density.

II. SYSTEM MODEL

In this section, we present the network architecture and assumptions used for modeling the cooperative multi-hop network. Consider a strip-shaped 2D network with a finite node density where the node locations are random as shown in Fig. 1. A hop or level is formed opportunistically by a group of decode-and-forward (DF) nodes that successfully decode the signal, transmitted by a source node or a group of nodes in the previous level. The DF nodes retransmit the same signal to the nodes ahead in the next time slot. Initially, for the first time slot, the source node transmits the signal, which is received by a group of nodes in the proximity and a subset of nodes decodes the message successfully depending upon transmit power, decoding threshold and nodes density. The nodes that successfully decode the signal become members of the first level (or hop). The DF nodes at level 1 transmit the same

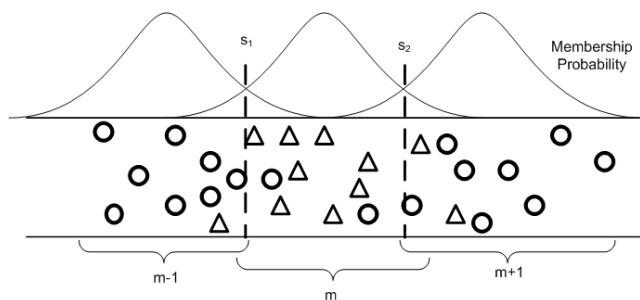


FIGURE 2. Formation of levels along with membership probability.

signal in the next time slot cooperatively and level 2 is formed. This process continues and subsequent levels are formed until the destination is reached or the message is broadcasted to the entire network. A node can successfully decode the signal, transmitted by a group of nodes in the previous level, if the accumulated received power is greater than the decoding threshold. The received power at each node is a RV, dependent upon channel impairments. It can be noticed that during the entire transmission process, a hop is formed opportunistically and that there are no fixed boundaries between the nodes of two levels as shown in Fig. 2.

The problem at hand is to find the coverage range of this network given the nodes transmit with a fixed power. However, to solve this problem, we intend to find the success probability of an arbitrary node in the network. This success probability is then used to characterize the success of one hop, and subsequently the probability of successful delivery of message for arbitrary number of hops.

Let the total length of the network be divided into multiple hops, such that the average hop distance is denoted by μ . Let ϕ denotes a homogeneous Poisson point process (PPP) on a hop with intensity $\tilde{\lambda}$ such that the average number of nodes in a hop is $\tilde{\gamma} = \tilde{\lambda}|S|$, where $|S|$ denotes the area of a single hop. The probability of having k_n nodes in one hop is thus given by

$$\mathbb{P}(\phi(S) = k_n) = \exp(-\tilde{\lambda}|S|) \frac{(\tilde{\lambda}|S|)^{k_n}}{k_n!}. \tag{1}$$

Generally, each level or hop contains a random number of nodes and the number of hops required to deliver a message to a given distance is dependent upon network parameters. The uniform distribution of the nodes makes the assumption of homogeneous PPP suitable as it allows to model the random number of nodes in a level as compared to a fixed number of nodes per hop modeled generally with a binomial point process [13].

The multiple copies of the same signal received by a node, transmitted by a group of nodes in the previous level, are assumed to be synchronous over independent fading channels [14] and are transmitted with equal transmit power. A virtual multiple-input single-output (MISO) is formed as shown in Fig. 3, which gives rise to spatial diversity and hence more reliability. A hop is said to be successful, if there

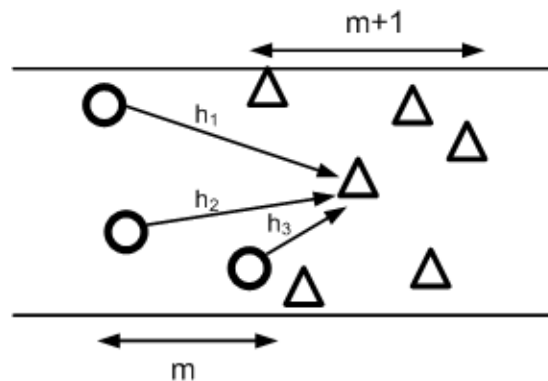


FIGURE 3. Transmission of signal from one hop to another without a fixed hypothetical boundary. A single receiving node constitutes a MISO scenario.

exists at least one DF node in the next hop provided the DF nodes in the previous level relayed the signal. The intensity of the DF nodes at level m is $\lambda = \tilde{\lambda}P_s^m$, where P_s is the success probability of a node [15]. The Sections III and IV of this manuscript deal with the calculation of this probability. Because of random node locations and random hop boundaries, a node in the network can be a part of different group of DF nodes or levels, hence the membership of a node to a particular level becomes random, which we discuss in the following section.

A. MEMBERSHIP OF A NODE

It can be noticed that because of random channel characteristics, a node can be part of many levels in different CT sessions. The tendency of the nodes to be in the same hop or level in subsequent iterations of the CT is higher if the nodes are present around the center of a level and the tendency decreases gradually for the nodes located near the boundary. The path loss is the main factor in governing such behavior of the nodes. The nodes present near the boundary of a hop can become part of the adjacent hop due to the lower path loss as compared to the path loss of the nodes present around the center of the hop. The membership probability of a node that it transmits in hop m is different for every other node of the hop as shown in Fig. 2. For instance, a node located near the boundary of hop, $m - 1$, can become a member of the next hop, m , provided it has not transmitted the signal before and successfully decoded the signal in next time slot. The nodes located at point s_1 have almost equal probability of becoming a member of hop $m - 1$ or m . A node has a non-zero probability of becoming a member of any level unless it has not transmitted before. The Kolmogorov-Smirnov (K-S) [16] test is used to check the similarity of the membership probability distribution to known distributions.

Monte-Carlo simulations are used to collect the data for the membership probability and K-S test is applied to find a similar distribution. For the simulation purpose, we consider a strip-shaped network of length 300 and width 8 in which

nodes are distributed uniformly. A source node is placed at the start of the network and it broadcasts the signal. Every other node that receives the signal and able to successfully decode it, based on threshold, $\tau = 0.04$, will transmit the signal in the next time slot. The DF nodes that transmit the signal at next time slot form level 1. The nodes with received power greater than τ and which are not part of the previous level (or levels), form next level. This process continues till the signal is broadcasted to the entire network. We observe the decoding pattern of the nodes in the subsequent levels formed at a later stage of the process. This process is repeated N times for two different intensities and independent data samples $\{\xi_1, \xi_2, \dots, \xi_N\}$ of membership are collected with cumulative density function (CDF) $F_1(\xi)$. The hypothesized CDF with which K-S test is performed is $F_0(\xi)$ and subsequently the null hypothesis which requires testing is given as

$$H_0 : F_1 = F_0. \tag{2}$$

The empirical CDF is calculated from N independent and identically distributed (I.I.D.) samples, given as

$$\hat{F}_1(\xi) \triangleq \frac{1}{N} \sum_{n=1}^N \mathbb{I}(\xi_n \leq \xi), \tag{3}$$

where $\mathbb{I}(\cdot)$ is the indicator function, which is 1 if the condition $(\xi_n \leq \xi)$ is satisfied and 0 otherwise. The maximum difference between the empirical CDF and hypothesized CDF is a statistic used for goodness-of-fit known as K-S statistic, given by [22]

$$D_f \triangleq \sup_{\xi} |\hat{F}_1(\xi) - F_0(\xi)|, \tag{4}$$

where \sup is the supremum operator, which is the least upper bound of a subset or a set. Usually, (4) is calculated as

$$\hat{D}_f = \max_i |\hat{F}_1(\xi_i) - F_0(\xi_i)|, \tag{5}$$

for samples $\{\xi_i\}$. Another input to the K-S test is the significance level, $\hat{\alpha}$, which is the probability of rejecting the null hypothesis given that the two distributions are same, defined as

$$\hat{\alpha} \triangleq \mathbb{P}(D_f \geq \hat{c} | H_0), \tag{6}$$

where \hat{c} is the critical value dependent upon the significance level and sample size. The values of \hat{c} are given in tabular form in [16]. The null hypothesis is accepted if $\hat{D}_f \leq \hat{c}$, i.e., $F_1 = F_0$ and rejected otherwise.

The K-S test is performed with $N = 3000$ and $\hat{\alpha} = 0.05$ for different known distributions and results are summarized in the Table 1. The critical value, \hat{c} , is found to be 0.0246. It can be noticed that for the Gaussian distribution, $\hat{D}_f < \hat{c}$ and H_0 is accepted for both intensities. Hence the membership probability distribution can be modeled with a Gaussian distribution with some mean and variance based on the K-S statistics. The length of the hop or level controls the variance and mean is dependent upon the center of the hop. ¹

¹The distribution of membership functions of nodes in such OLA networks is also found to be Gaussian, e.g., [3] and [10].

TABLE 1. K-S test for membership probability.

Distribution name	$\hat{D}_f = \max_i \hat{F}_1(\xi_i) - F_0(\xi_i) $	
	Intensity = 0.0833	Intensity = 0.2083
Central chi-squared	0.5540	0.5995
Gaussian	0.0129	0.0214
Rayleigh	0.2800	0.3800
Weibull	0.0285	0.0336
Gamma	0.0395	0.0225

B. RECEIVED POWER

Let $\phi(S_m)$ denotes the number of DF nodes at a level m , then the received power at any node j at level $m + 1$ is given as

$$P_{r_j}(m + 1) = P_t \sum_{i \in \phi(S_m)} \frac{h_{ij}}{d_{ij}^\alpha}, \tag{7}$$

where P_t represents the transmitted power, h_{ij} denotes the effects of Rayleigh flat fading modeled with the unit mean exponential RV, d is the Euclidean distance between node i and j of two different levels and α is the path loss exponent. To calculate the CR of the network, m -hop success probability needs to be calculated, which is dependent upon the one-hop success probability and to calculate one-hop success probability for a virtual MISO case, the sum of the ratio of an exponential RV and the distance distribution is required. The distribution of the Euclidean distance between the nodes of the two adjacent levels is derived in the following section.

III. DISTANCE DISTRIBUTION

In this section, we derive the distribution of the random distance between a pair of nodes in adjacent levels. The nodes in one level communicate with the nodes in the next level, where nodes in each level are modeled by two independent PPPs. A distance distribution between two nodes, which are part of two distinct PPPs, needs to be derived. In other words, a distance distribution between two nodes of two PPPs is required, which is different compared to the distance distribution between nodes of a single PPP [17], [18]. As shown in Fig. 1, the network has a fixed vertical length and extends in the horizontal dimension. The nodes are distributed uniformly in the 2D network in both directions but the formation of levels changes the node distribution in horizontal direction with respect to a level or hop as shown in 2.

It follows from the membership probability that at a level, the nodes in the horizontal direction are concentrated around the center of the level and stretches in the outward direction, whereas vertical distribution of the nodes is not affected and they follow uniform distribution. The candidate node locations within one of the levels is modeled with random variables (RV). The horizontal component is modeled with

normal RV X given by

$$f_X(x) = \frac{1}{\sigma\sqrt{2\pi}} \exp\left(-\frac{(x-\nu)^2}{2\sigma^2}\right), \quad (8)$$

where ν is the mean of the normal distribution representing the center of a level and σ is the standard deviation characterizing the size of the level. On the other hand, uniform distribution is used to model the vertical component, given by

$$f_Y(y) = \begin{cases} \frac{1}{B}, & \text{if } 0 \leq y \leq B, \\ 0, & \text{otherwise,} \end{cases} \quad (9)$$

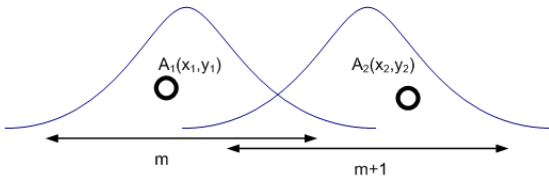


FIGURE 4. A realization of a pair of nodes placed randomly in adjacent levels.

where B is the width of the strip-shaped network. These two RVs completely describe the location of a node in one level. Let $A_1(x_1, y_1)$ and $A_2(x_2, y_2)$ be the two random nodes in adjacent levels at positions $x_i, y_i; i \in \{1, 2\}$ as shown in Fig. 4, then the Euclidean distance between two nodes is given by

$$d = \sqrt{(x_2 - x_1)^2 + (y_2 - y_1)^2}. \quad (10)$$

In (10), $x_i \in X_i$ and $y_i \in Y_i \forall i = \{1, 2\}$, where $X_i \sim N(\nu_i, \sigma^2)$ and $Y_i \sim U[0, B]$. If the means and variances of X_1 and X_2 are (ν_1, σ^2) and (ν_2, σ^2) respectively, then the difference between two normal RVs $X_2 - X_1$ is also a normal RV O , whose PDF is given as

$$f_O(o) = \frac{1}{\Delta\sqrt{2\pi}} \exp\left(-\frac{(o-\mu)^2}{2\Delta^2}\right), \quad (11)$$

where $\mu = \nu_2 - \nu_1$ with standard deviation $\Delta = \sqrt{2\sigma^2}$. Usually $2\sigma = \mu/2$, as 95% of the data in normal distribution are contained within 2 standard deviations. However from (10), the squared difference of RVs, i.e., $(X_2 - X_1)^2$ is desired, which for normal RVs is given as a non-central chi-squared RV. Limiting this distribution to one degree of freedom will provide the distribution of the squared normal RV, $T = O^2$, given as

$$f_T(t) = \frac{1}{2\sqrt{2\pi\Delta^2 t}} \exp\left(-\frac{t+\mu^2}{2\Delta^2}\right) \times \left[\exp\left(\sqrt{\frac{\mu^2 t}{\Delta^4}}\right) + \exp\left(-\sqrt{\frac{\mu^2 t}{\Delta^4}}\right) \right], \quad t \geq 0. \quad (12)$$

Similarly, for the y -component, let $P = Y_2 - Y_1$ and its probability density function (PDF) is given as

$$f_P(p) = \begin{cases} \frac{1}{B^2} (B+p), & \text{if } -B < p \leq 0, \\ \frac{1}{B^2} (B-p), & \text{if } 0 < p \leq B, \\ 0, & \text{otherwise.} \end{cases} \quad (13)$$

The distribution of $L = P^2$ is then given as [19]

$$f_L(l) = \begin{cases} \frac{1}{B\sqrt{l}} - \frac{1}{B^2}, & \text{if } 0 < l \leq B^2, \\ 0, & \text{otherwise.} \end{cases} \quad (14)$$

The distribution of the squared Euclidean distance is thus equal to the distribution of the sum of RVs T and L , having distributions given in (12) and (14), respectively. However, this addition of RVs is not straight forward, owing to the non linear terms in (14). Hence the distribution of RV L is approximated with another distribution, complying with the features of L as shown in the following Lemma.

Lemma 1: The distribution of the square of the difference between two uniform RVs can be approximated by a central chi-squared distribution with standard deviation, $\nu = 0.408B$, given as

$$f_G(g) = \frac{1}{\sqrt{2\pi\nu^2 g}} \exp\left(-\frac{g}{2\nu^2}\right), \quad g \geq 0. \quad (15)$$

Proof: A two step process is used to approximate the distribution of the RV L to another distribution. In the first step, method of moments is used to match the moments of RV L to that of Central Chi-squared RV with one degree of freedom. It models the squared sum of zero mean normal RVs. Since the distribution of L involves only one parameter, therefore, matching only the first moment is enough. The first moment of L is calculated as

$$\mathbb{E}[L] = \int_0^{B^2} l f_L(l) dl = \frac{B^2}{6}, \quad (16)$$

where $\mathbb{E}[\cdot]$ is the expected value. The expected value of Central Chi-squared RV, G , with one degree of freedom is calculated as

$$\mathbb{E}[G] = 2\nu^2 \frac{\Gamma(1+1/2)}{\sqrt{\pi}}, \quad (17)$$

where ν is the standard deviation of the zero mean normal RV and $\Gamma(\cdot)$ is the gamma function. Matching the moments and solving the equations provides the value of ν depending upon the width, B , of the strip-shaped network, given as

$$\nu = 0.408B. \quad (18)$$

In the second step, the K-S test is used for goodness-of-fit. The $N = 2500$ I.I.D. samples $\{\xi_1, \xi_2, \dots, \xi_N\}$ of RV L are observed and empirical CDF, \hat{F}_L , is calculated using (3). The hypothesized CDF is that of Central Chi-squared distribution, F_G . The critical value is found to be $\hat{c} = 0.0326$ against the level of significance $\hat{\alpha} = 0.01$. The null hypothesis is

$$H_0 : F_L = F_G. \quad (19)$$

The two values of the K-S statistics, \hat{D}_f , calculated using (5) are

$$\begin{aligned} \hat{D}_f &= 0.0288 \text{ for } B = 5, \\ \hat{D}_f &= 0.0238 \text{ for } B = 10. \end{aligned} \quad (20)$$

It can be noticed that $\hat{D}_f < \hat{c}$ for both values and H_0 cannot be rejected. Hence the new distribution for RV L approximated with RV G is given in (15). ■

The squared Euclidean distance now becomes the sum of a non-central chi-squared RV from (12) and a central chi-squared RV from (15), for which we define $Z = T + G$. Note that T and G are independent RVs and the distribution of their sum is given as [20]

$$\begin{aligned} f_Z(z) &= \frac{1}{2\Delta v} \exp\left(-\frac{z + \mu^2}{2\Delta^2}\right) \sum_{i=0}^{\infty} \frac{\Gamma(1/2 + i)}{i! \Gamma(1/2)} \\ &\times \left(\frac{\sqrt{z}(v^2 - \Delta^2)}{\mu v^2}\right)^i I_i\left(\frac{\sqrt{z}\mu}{\Delta^2}\right), \quad z \geq 0, \end{aligned} \quad (21)$$

where $\Gamma(\cdot)$ denotes the gamma function and $I_i(\cdot)$ is the modified Bessel function of the first kind.

The distribution of the received power, using the distance distribution derived above, becomes prohibitive as (21) involves infinite summation terms. Therefore, to analytically derive an expression for the PDF of the received power, we need to approximate (21) with some tractable expression. Using the moments matching method, we approximate the squared distance distribution to another function with similar properties and complying with the effects of the parameters μ , Δ and v of RV Z , as shown in the following Lemma.

Lemma 2: The distribution of the Euclidean distance raised to power α between a pair of nodes in two adjacent levels as shown in Fig. 4, can be approximated by a Weibull distribution with shape parameter, c , and scale parameter, χ , such that

$$f_Q(q) = \frac{c}{\chi^c} q^{c-1} \exp\left[-\left(\frac{q}{\chi}\right)^c\right], \quad q \geq 0, \quad (22)$$

where $\chi = \zeta^{\alpha/2}$, $c = 2k/\alpha$ and the values of ζ and k are given in (26.)

Proof: A similar two step process as used in Lemma 1, is used to approximate the squared distance distribution, Z . Firstly method of moments is applied to match the moments of RV Z to moments of Weibull RV, W . Weibull distribution is based on two parameter, i.e., shape parameter, k , and scale parameter, ζ . The first moment of Z is calculated as

$$\mathbb{E}[Z] = \int_0^{\infty} z f_Z(z) dz = \mu^2 + \Delta^2 + v^2. \quad (23)$$

and the second moment is

$$\begin{aligned} \mathbb{E}[Z^2] &= \int_0^{\infty} z^2 f_Z(z) dz \\ &= \mu^4 + 3\Delta^4 + 3v^4 + 2\Delta^2 v^2 + 2\mu^2 (v^2 + 3\Delta^2). \end{aligned} \quad (24)$$

The first two moments of Weibull RV, W , are

$$\begin{aligned} \mathbb{E}[W] &= \zeta \Gamma\left(1 + \frac{1}{k}\right), \\ \mathbb{E}[W^2] &= \zeta^2 \Gamma\left(1 + \frac{2}{k}\right). \end{aligned} \quad (25)$$

Proceeding with the algorithm of moments matching, we get two non-linear equations. Simplifying the equations we get

$$\begin{aligned} \zeta &= \frac{\mu^2 + \Delta^2 + v^2}{\Gamma(1 + 1/k)}, \\ \frac{\Gamma(1 + 2/k)}{[\Gamma(1 + 1/k)]^2} &= 1 + \frac{4\mu^2 \Delta^2 + 2\Delta^2 + 2v^2}{(\mu^2 + \Delta^2 + v^2)^2}. \end{aligned} \quad (26)$$

The value ζ is dependent upon the value of k , whereas the value of k is calculated numerically. The new distribution of the squared Euclidean distance is given as

$$f_W(w) = \frac{k}{\zeta^k} w^{k-1} \exp\left[-\left(\frac{w}{\zeta}\right)^k\right], \quad w \geq 0. \quad (27)$$

In the second step, the K-S test is used to show that the Weibull distribution closely matches the squared distance distribution, Z . The empirical CDF, \hat{F}_Z , of the samples $\{\xi_1, \xi_2, \dots, \xi_N\}$ of the squared distance is calculated using (3). The critical value, \hat{c} , for level of significance, $\hat{\alpha} = 0.01$, and $N = 2500$ samples is found to be 0.0326. The hypothesized CDF is of Weibull distribution, F_W , and the null hypothesis is

$$H_0 : F_Z = F_W. \quad (28)$$

The K-S test is conducted for two set of parameters, i.e., $\{B = 5, \mu = 5, \Delta = 2.83\}$ and $\{B = 3, \mu = 4, \Delta = 1.41\}$ and K-S statistics, \hat{D}_f , is calculated using (5) for each set, given as

$$\begin{aligned} \hat{D}_f &= 0.0256 \text{ for } B = 5, \mu = 5, \Delta = 2.83, \\ \hat{D}_f &= 0.0212 \text{ for } B = 3, \mu = 4, \Delta = 1.41. \end{aligned} \quad (29)$$

H_0 cannot be rejected as $\hat{D}_f < \hat{c}$ for each set. Hence Weibull distribution closely matches the squared distance distribution and can be used to approximate the squared distance distribution.

In (7), distance is raised to path loss exponent, α , so the distribution of the distance raised to power, α , where $d^\alpha \in Q$ and $Q = W^{\alpha/2}$, given as

$$f_Q(q) = \frac{2}{\alpha} q^{\frac{2}{\alpha}-1} f_W(q^{\frac{2}{\alpha}}). \quad (30)$$

Hence the distribution of the Euclidean distance raised to power, α , for the network shown in Fig. 4, is also Weibull given in (22). ■

This distance distribution is used to find the received power distribution in a virtual MISO case in the following section.

IV. MISO NETWORK

The received power for the virtual MISO network as shown in Fig. 3, is the sum of ratio of an exponential RV, H , and a Weibull RV, Q , where the sum is dependent upon the number of the DF nodes in the previous level which are distributed according to a PPP. As in (7), the received power is given as

$$P_{r_j}(m + 1) = P_t \sum_{i \in \phi(S_m)} \frac{H_i}{Q_i} \triangleq P_t \sum_{i \in \phi(S_m)} R_i, \quad (31)$$

where $\phi(S_m)$ is the number of the DF nodes in level m . To study such networks, the PDF of the received power needs to be determined by self-convolving the distribution of RVs R_i as they are independent and identically distributed (I.I.D). The PDF of a single RV, R , is given as [21]

$$f_R(r) = \chi \sum_{n=0}^{\infty} \frac{1}{n!} \Gamma\left(\frac{1+c+n}{c}\right) (-r\chi)^n. \quad (32)$$

We consider the following theorem for finding the coverage probability of a virtual MISO link.

Theorem 1 (Coverage Probability of a Virtual MISO Link): *If nodes in each level are distributed according to a PPP with mean $\tilde{\gamma} = \tilde{\lambda}|S|$ and the mean of the DF nodes in the previous level n is $\gamma = \lambda|S|$, then the coverage probability, P_s , for a random node in the next level $n + 1$ is given by*

$$P_s = 1 - \exp(-\gamma) \left[\sum_{m=0}^{\infty} \frac{(\gamma\chi)^m}{m!} \sum_{a_1=0}^{\infty} \sum_{a_2=0}^{\infty} \dots \sum_{a_m=0}^{\infty} \frac{(\tau/P_t)^{a_1+a_2+\dots+a_m+m}}{(a_1+a_2+\dots+a_m+m)!} \times \prod_{i=1}^m \Gamma\left(\frac{1+c+a_i}{c}\right) (-\chi)^{a_i} \right]. \quad (33)$$

Proof: The self-convolution of the distribution of the ratio RVs, R , is reduced to their product in frequency domain, given as

$$\mathcal{L} \left[\underset{z=1}{*}^{k_n} f_{R_z}(r_z) \right] = \prod_{z=1}^{k_n} F_z(s) = (F(s))^{k_n}, \quad (34)$$

where $*$ denotes the convolution operator, \mathcal{L} is the Laplace operator and $F(s)$ is the Laplace transform of $f_R(r)$, given as

$$F(s) = \chi \sum_{n=0}^{\infty} \frac{1}{n!} \Gamma\left(\frac{1+c+n}{c}\right) (-\chi)^n \frac{1}{s^{n+1}}. \quad (35)$$

The value of RV, k_n , in (34) depends upon the number of nodes in the previous level. We calculate the expected value of $(F(s))^{k_n}$ with respect to the Poisson RV, k_n , with mean $\gamma = \lambda|S|$ as

$$G(s) = \mathbb{E} \left[(F(s))^{k_n} \right] = \sum_{k_n=0}^{\infty} \frac{(\lambda|S|)^{k_n} \exp(-\lambda|S|)}{k_n!} (F(s))^{k_n}. \quad (36)$$

After some mathematical manipulation, we obtain

$$G(s) = \exp \left(\lambda|S|\chi \sum_{n=0}^{\infty} \frac{1}{n!} \Gamma\left(\frac{1+c+n}{c}\right) (-\chi)^n \frac{1}{s^{n+1}} \right) \times \exp(-\lambda|S|). \quad (37)$$

The above function is quite complex and direct inverse Laplace transform is prohibited in closed-form, so we expand the first exponential function in (37) with a Taylor series such that

$$G(s) = \sum_{m=0}^{\infty} \left(\lambda|S|\chi \sum_{n=0}^{\infty} \frac{1}{n!} \Gamma\left(\frac{1+c+n}{c}\right) (-\chi)^n \frac{1}{s^{n+1}} \right)^m \times \exp(-\lambda|S|). \quad (38)$$

Simplifying the above function for m , we get

$$G(s) = \left[\sum_{m=0}^{\infty} \frac{(\lambda S \chi)^m}{m!} \sum_{a_1=0}^{\infty} \dots \sum_{a_m=0}^{\infty} \frac{1}{s^{a_1+a_2+\dots+a_m+m}} \times \prod_{i=1}^m \Gamma\left(\frac{1+c+a_i}{c}\right) (-\chi)^{a_i} \right] \exp(-\lambda|S|). \quad (39)$$

The PDF of the receive power, P_r , is found by taking the inverse Laplace transform of the $G(s)$, given as

$$f_{P_r}(p_r) = \exp(-\lambda|S|) \left[\sum_{m=0}^{\infty} \frac{(\lambda|S|\chi)^m}{m!} \sum_{a_1=0}^{\infty} \sum_{a_2=0}^{\infty} \dots \sum_{a_m=0}^{\infty} \frac{(p_r)^{a_1+a_2+\dots+a_m+m-1}}{(a_1+a_2+\dots+a_m+m-1)!} \times \prod_{i=1}^m \Gamma\left(\frac{1+c+a_i}{c}\right) (-\chi)^{a_i} \right]. \quad (40)$$

The integration of the above expression will yield the CDF, $F_{P_r}(p_r)$, of the received power and outage probability, P_o , is obtained by evaluating the CDF at $F_{P_r}(\tau/P_t)$. The coverage probability given in (33) is calculated as

$$P_s = \mathbb{P}(P_r \geq \tau) = 1 - \mathbb{P}(P_r \leq \tau) = 1 - P_o. \quad (41)$$

The coverage probability is inversely proportional to χ , which specifies the distance distribution and directly proportional to the node intensity. The coverage probability, P_s , is same for each node of any one level. The one-hop success probability, P_{one} , is calculated using the coverage probability, given as

$$P_{one} = \mathbb{P}(k_n \geq 1) = 1 - \mathbb{P}(k_n = 0) = 1 - \exp(-\lambda|S|P_s). \quad (42)$$

The CR and m -hop success probability of the network, while maintaining a QoS, η , is calculated using the coverage probability, P_s , which is unique for different set of the network parameters (P_t , γ , τ , etc.). If the average number of the

DF nodes in the first level after transmission is γP_s , and the average number of the DF nodes at level m is γP_s^m , then the m -hop success probability is calculated as

$$\mathbb{P}(k_n \geq 1) = 1 - \exp(-\gamma P_s^m). \quad (43)$$

The QoS, η , which is the desired m -hop success probability, acts as an upper bound on m -hop success probability to calculate the number of the hops which the signal traverses, i.e., $\mathbb{P}(k_n \geq 1) \geq \eta$. The maximum hop count is calculated by comparing m -hop success probability with η , given as

$$m \leq \frac{\ln[-\ln(1-\eta)/(\lambda|S|)]}{\ln P_s}. \quad (44)$$

The average value of CR can then be calculated as

$$CR = m\mu. \quad (45)$$

V. THINNING OF POISSON PROCESS TO ACHIEVE ENERGY EFFICIENCY

The energy efficiency of the system can be improved by limiting the number of nodes per level that relay the information. Usually for a network with a high node density, the transmissions from all the DF nodes of one level are not required for the formation of the next level. Similar results can be achieved by having a limited node participation at different hops. The nodes present near the source or the boundary of previous level have much higher received powers owing to less average path loss and when they transmit to the next level nodes, their transmissions have little or no effect on the decoding of the nodes of next level because of large path loss between them and the next level nodes. Limiting such nodes from transmission to the next level and allowing only those nodes which are nearer to the next level boundary, conserves a significant amount of energy. A threshold based criteria is used to limit such nodes, i.e., only those nodes are allowed to transmit whose SNR margin is greater than decoding threshold and less than an upper bound threshold. Hence in this section, we devise a method to improve the energy efficiency of the network by having limited node participation.

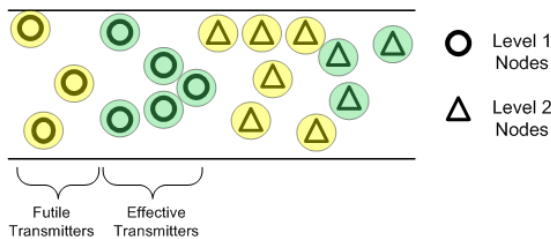


FIGURE 5. Two subsets of transmitters in the ad hoc network.

The nodes in one level are divided into two subsets of transmitters based on the above criteria, i.e., effective transmitters and futile transmitters as shown in Fig. 5. The two subsets of the transmitters do not need to be of equal sizes. Their sizes can vary, however, increasing the number of nodes in

one subset decreases the number of nodes in the other and vice versa. The size of two subsets can be made dependent upon the quality of service (QoS), η , and other network parameters. The QoS in this case can be defined as the minimum end-to-end success probability required for the network. We devise the thinning of OLA (Th-OLA) algorithm, which is derived from the basic OLA with additional constraint for transmission that the nodes must be closer to the boundary of the next level. This type of situation can be attributed to a larger rectangular area, where nodes are distributed according to a PPP, but for transmission purpose, only the nodes of a smaller rectangular area are selected as shown in Fig. 6. We consider the following the theorem for the thinning of PPP.

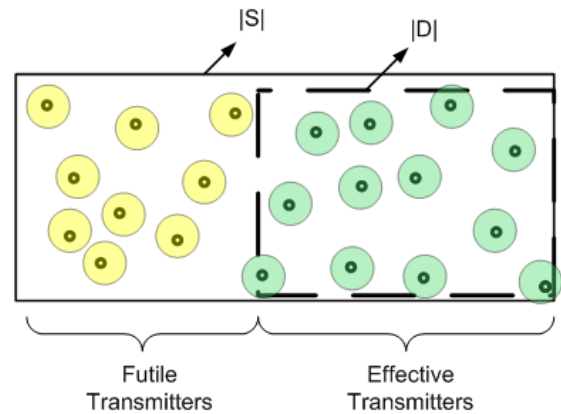


FIGURE 6. Depiction of the process of Thinning of PPP.

Theorem 2: If nodes are distributed according to a PPP, ϕ , with intensity λ in an area $|S|$ and the thinning function permits only j nodes located in the area $|D|$, where $|D| \subseteq |S|$ almost surely, then the distribution of the nodes in area $|D|$ still follows another PPP, $\bar{\phi}$, with same intensity λ , such that

$$\mathbb{P}(\bar{\phi}(D) = j) = \exp(-\lambda|D|) \frac{(\lambda|D|)^j}{j!}. \quad (46)$$

Proof: Let $\phi(S)$ be the PPP with mean $\lambda|S|$ and $\bar{\phi}(D)$ be the process obtained after thinning. The distribution of $\bar{\phi}(D)$ can be calculated as

$$\mathbb{P}(\bar{\phi}(D) = j) = \sum_{k_n=j}^{\infty} \mathbb{P}(\phi(S) = k_n) \mathbb{P}(\bar{\phi}(D) = j | \phi(S) = k_n), \quad (47)$$

where k_n is the number of the nodes in the original PPP and j denotes the number of nodes in the new PPP obtained after thinning. Since the nodes are distributed uniformly, we calculate the conditional probability of finding a node in $\bar{\phi}(D)$ given that $\phi(S) = 1$ as

$$\mathbb{P}(\bar{\phi}(D) = 1 | \phi(S) = 1) = \frac{|D|}{|S|}. \quad (48)$$

The conditional probability of $\bar{\phi}(D) = j$ given that $\phi(S) = k_n$ is given as

$$\mathbb{P}(\bar{\phi}(D) = j | \phi(S) = k_n) = \binom{k_n}{j} \left(\frac{|D|}{|S|}\right)^j \left(1 - \frac{|D|}{|S|}\right)^{k_n-j} \quad (49)$$

Using the above expression in (47), we get

$$\begin{aligned} \mathbb{P}(\bar{\phi}(D) = j) &= \sum_{k_n=j}^{\infty} \exp(-\lambda|S|) \frac{(\lambda|S|)^{k_n}}{k_n!} \\ &\times \binom{k_n}{j} \left(\frac{|D|}{|S|}\right)^j \left(1 - \frac{|D|}{|S|}\right)^{k_n-j} \\ &= \exp(-\lambda|S|) \frac{(\lambda|D|)^j}{j!} \\ &\times \sum_{k_n=j}^{\infty} \frac{[\lambda|S|(1 - |S|^{-1}|D|)]^{k_n-j}}{(k_n - j)!}. \end{aligned} \quad (50)$$

After some mathematical manipulations, we obtain

$$\begin{aligned} \mathbb{P}(\bar{\phi}(D) = j) &= \exp(-\lambda|S|) \frac{(\lambda|D|)^j}{j!} \\ &\times \exp\left[\lambda|S|(1 - |S|^{-1}|D|)\right] \\ &= \frac{(\lambda|D|)^j}{j!} \exp(-\lambda|D|). \end{aligned} \quad (51)$$

Hence the thinning process directly reduces the effective hop area, whereas the intensity of the nodes remains the same with same distribution. ■

The distance between the nodes of two consecutive hops is modeled with (22) with reduced mean, $\tilde{\mu}$, and reduced standard deviation, $\tilde{\Delta}$, as the effective transmit area of a hop reduces, however, Theorem 1 can be used to analyze the Th-OLA. The value of $\tilde{\mu}$ is always less than μ as the effective hop area cannot be greater than the original one.

Let the number of the nodes that relay the signal at level i is $k_{n,i}$ in basic OLA and the number of the nodes that relay the signal after thinning process is j_i . Then the total transmit power for basic OLA in transmitting the signal up to m hops while maintaining a QoS is $P_t \sum_{i=0}^m k_{n,i}$, which is dependent upon the RV k_n and the ergodic mean of the total energy consumed is $P_t m \gamma_b$, where γ_b is the average number of nodes per hop for basic OLA. Similarly, the total transmit energy for thinned OLA is $P_t \sum_{i=0}^m j_i$ and its mean value is $P_t m \gamma_t$, where γ_t is the average number of nodes per hop for Th-OLA. The fraction of energy saved (FES) can be calculated as

$$\begin{aligned} FES &= 1 - \frac{\text{Total energy of the Th-OLA}}{\text{Total energy of the basic OLA}} \\ FES &= 1 - \frac{P_t m \gamma_t}{P_t m \gamma_b} \\ &= 1 - \frac{\gamma_t}{\gamma_b}. \end{aligned} \quad (52)$$

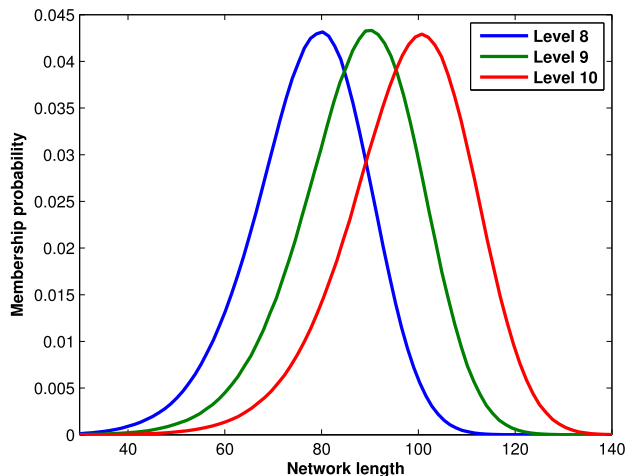


FIGURE 7. Membership probability in three adjacent levels for $B = 8$, $\tau = 0.04$, $\alpha = 2$.

VI. RESULTS AND DISCUSSION

In this section, we validate our analytical models that characterize the performance of a virtual MISO network in terms of the coverage probability, one-hop success probability, coverage range and the energy efficiency of the network. We calculate the membership probability of the three subsequent levels for a network of length 200, width 8 and intensity 0.1125 as shown in Fig. 7 by repeating the process for $1e5$ iterations. It can be observed that the node membership follows a Gaussian distribution and the membership probability for the three adjacent levels are almost similar with similar mean and standard deviation. This behavior links to the quasi-stationary phenomenon, which informs that a steady-state is reached when a wave (of transmission) traverses the entire network [10].

We now compare the distribution of the squared Euclidean distance derived from computer simulations with the Weibull distribution derived in Section III. For the sake of computer simulations, two nodes are positioned randomly in adjacent levels and x coordinates of node 1 and node 2 are generated according to Gaussian distributions $N(v_1, \sigma)$ and $N(v_2, \sigma)$, respectively, where $\mu = v_2 - v_1$. The parameter μ specifies the hop distance and y coordinates of both nodes are generated according to a uniform distribution, i.e., $U(0, B)$. The squared Euclidean distance is calculated between these two nodes and the process is repeated over $1e6$ iterations to calculate the resulting PDF. It can be seen from Fig. 8 that the analytical results for different values of the hop distance, μ , closely match the simulation results. Hence, the Weibull distribution in (27) provides a good approximation for the squared Euclidean distance. Note that a large value of μ specifies that the two levels are farther apart from each other. Hence the values of the PDF on the ordinate become smaller.

Fig. 9 validates the findings of Theorem 1 by comparing it to that of simulations. For simulation purpose, a random number of nodes is generated using a Poisson RV in one level

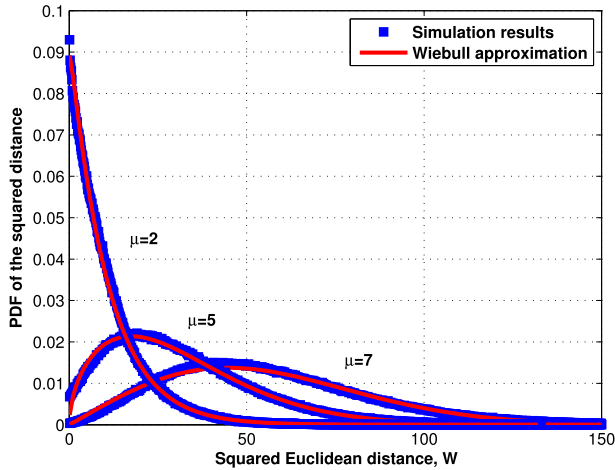


FIGURE 8. Comparison of the simulation distance distribution with the Weibull distribution for $B = 4$, $\Delta = 2$ and $\alpha = 2$.

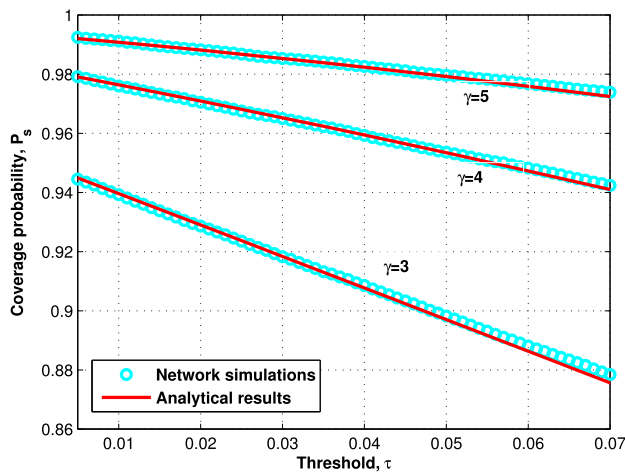


FIGURE 9. Comparison of the coverage probability of a node for MISO using analytical and simulation model for $B = 4.69$, $\mu = 1.17$, $\Delta = 1.45$, $P_t = 1$ and $\alpha = 2$.

and the received power at a node in the next level is calculated using (7) and compared with a decoding threshold, τ . The coverage probability at a node is calculated by repeating the process over $1e5$ iterations. The results are calculated for various values of τ and different average number of nodes, γ . The analytical model of the coverage probability requires infinite summation terms, however, two decimal point accuracy can be achieved with initial six terms. It can be noticed that the analytical model provides a close fit to the simulation model. Also we can infer the relationship between coverage probability of a node and the decoding threshold. Coverage decreases as we increase the threshold or decrease the number of nodes per hop. For instance, it can be seen that at $\tau = 0.04$, the coverage probability increases by 5.5% when γ is increased from 3 to 4. Whereas the increase in coverage probability is 2.1% when γ is increased from 4 to 5. Hence a diminishing trend can be observed.

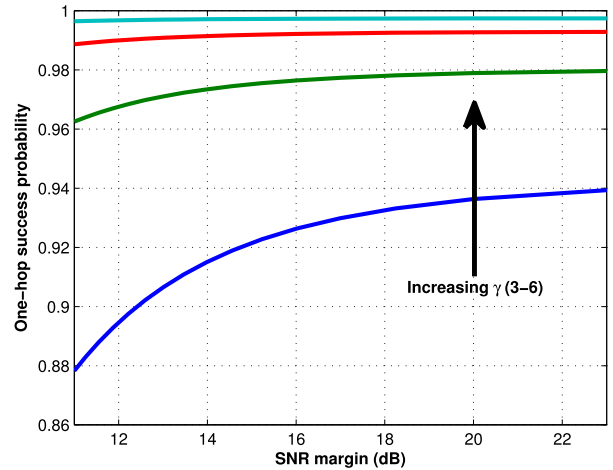


FIGURE 10. Effect of the average number of nodes on one-hop success probability with $\alpha = 2$, $\mu = 2.62$, $\Delta = 2.12$ and $B = 7.87$.

In Fig. 10, the one-hop success probability of the random network with different average number of nodes is plotted against the SNR margin, $\psi = P_t/\tau$. It can be observed that the one-hop success probability increases with the increasing node densities for a fixed SNR margin and it also increases as the SNR margin is increased for a fixed node density. It can be seen that the one-hop success probability curves seem to approach a limiting value with the increased SNR margin. This asymptotic limit trace back to the theory of PPP, as the number of nodes at level m can be zero with probability $\exp(-\gamma P_s^m)$, which amounts to a hop failure. These failures can be reduced by increasing the node intensities and/or hop area, which in turn reduces the void probability. Hence the node intensities play a vital role in achieving a certain one-hop success probability as compared to SNR margin.

TABLE 2. Coverage range.

QoS η	Case 1		Case 2	
	Analytical	Simulations	Analytical	Simulations
0.8	5.93	5.95	5.51	5.64
0.7	9.35	8.7	8.221	7.95
0.6	12.57	11	10.77	10.30
0.5	15.87	14.5	13.37	13.19
0.4	19.48	18.2	16.21	16.36
0.2	29.26	28.9	23.93	24.9

Table 2, validates our stochastic model by comparing the coverage range (CR) of a pure OLA network to that of the proposed analytical model. For pure OLA network, Monte-Carlo simulations are used. A strip-shaped network with random node locations is considered such that a source node is placed at the start of the network and it broadcasts the signal using OLA protocol discussed earlier. Once steady-state is reached, i.e., after reaching a particular hop, the hop distance, μ , between any two hops and average number of nodes, γ ,

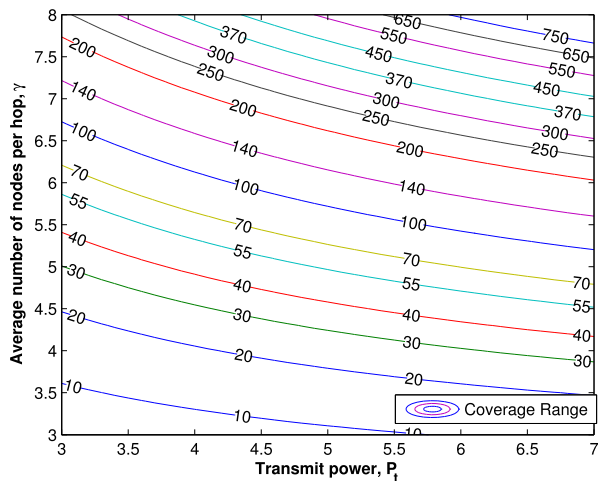


FIGURE 11. Coverage range for different values of transmit power, P_t , and average number of nodes, γ with $\mu = 4.05$, $\Delta = 1.27$, $B = 9.75$, $\eta = 0.8$ and $\tau = 0.2$.

per hop remain almost same. This process is repeated $1e4$ times and the CR is calculated for different values of the QoS after steady-state is reached. The following two cases are considered and findings of the simulation are compared with the analytical model:-

Case 1 : $\mu = 3.93$, $\gamma = 2.66$, $\tau = 0.08$, $P_t = 1$, $W = 4$

Case 2 : $\mu = 2.86$, $\gamma = 2.91$, $\tau = 0.16$, $P_t = 1$, $W = 4.69$

The analytical results obtained by using Theorem 1 and plugging values in (45) closely match the simulation results. Hence the proposed model can be seen effective in modeling a pure OLA network.

A contour plot of CR against the transmit power, P_t , and the average number of the nodes, γ , is shown in Fig. 11, for $\eta = 0.8$ and $\tau = 0.2$. It is observed that the same value of CR can be attained for different set of values of P_t and γ and a network designer can choose any set of parameters depending upon the network constraints and requirements. For instance, it can be seen that at $\gamma = 8$, the CR is increased by 278% when P_t is increased from 3 to 7. Whereas, the CR increases by 134% with $\gamma = 4$ for the same increase in transmit power.

We now focus on the results of the energy efficiency for OLA network. Fig. 12 shows the FES computed for different values of the CR while maintaining a QoS. For calculating the success probability of the Th-OLA, $\tilde{\mu}$ is used, however, CR is calculated using μ as hop length does not change. It can be seen that the FES decreases with the increasing CR for a particular γ but still a significant amount of energy can be conserved by using the proposed Th-OLA algorithm and network life can be extended. Since the effective diversity gain of the Th-OLA is less as compared to the basic OLA because of limited node participation, the CR of the Th-OLA is also small as compared to the basic OLA, however, to a particular CR, Th-OLA provides an energy efficient approach to achieve that CR. For instance, to achieve a CR of 375, Th-OLA with $\mu = 5$ and $\gamma = 14$ requires 50% less energy as compared to the basic OLA with $\mu = 5$ and $\gamma = 14$

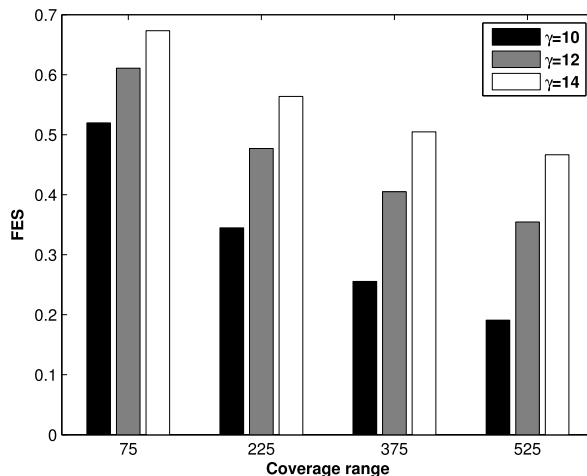


FIGURE 12. FES for three different values of γ with $\mu = 5$, $\psi = 14dB$, $B = 6$, $\eta = 0.8$, and $\Delta = 2$.

while maintaining the same QoS of 0.8. Hence Th-OLA is successful in saving the energy and extending the life time of the energy constraint networks.

TABLE 3. Effect of hop distance on FES.

γ	CR	Energy of Th-OLA (dB)		FES
		$\mu = 5$	$\mu = 8$	
10	120	21.2	20.3	0.1898
	200	24	23.2	0.1817
14	120	21	19.9	0.2085
	200	23.8	22.8	0.2043

Hop distance is an important factor in characterizing the energy requirements to achieve a particular CR. OLAs with different hop distances require different number of the hops to achieve the same CR. Similarly, Th-OLAs with different hop distances require different number of the hops to achieve the same CR, so the FES for the comparison of two Th-OLAs with different hop distances, i.e., μ_1 and μ_2 , is calculated with the modified version of (52), given as

$$FES = 1 - \frac{P_t m \gamma_{t1}}{P_t n \gamma_{t2}} = 1 - \frac{m \gamma_{t1}}{n \gamma_{t2}}, \quad (53)$$

where m and n are the number of hops required to achieve a particular CR with two different TH-OLAs of (γ_{t1}, μ_1) and (γ_{t2}, μ_2) , respectively. The Th-OLA with larger hop distance, $\mu = 8$, is compared to the Th-OLA with smaller hop distance, $\mu = 5$ and results are summarized in Table 3. These result are calculated for SNR margin, $\psi = 14dB$, with network width, $B = 6$, $\eta = 0.8$ and $\Delta = 2$. OLA with smaller hop distance can achieve a higher CR as compare to larger hop distance as increase in the hop distance increases the path loss attenuation. However, the network with larger hop distance, μ , provides more energy efficient approach in achieving a particular CR for a fixed γ and thus saves a considerable

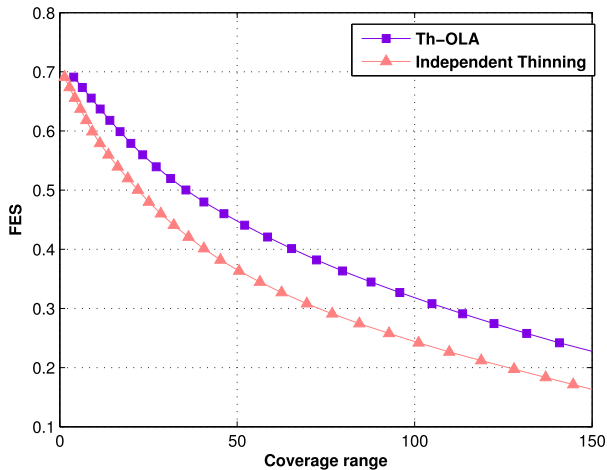


FIGURE 13. Comparison of the Th-OLA with the independent thinning process for $\psi = 14\text{dB}$, $\gamma = 8$, $\mu = 5$, $\Delta = 2$, $\eta = 0.8$ and $B = 6$.

amount of the energy at higher SNR margins. A large hop distance implies that the CR can be achieved in lesser number of the hops. Hence, the total energy requirements for larger hop distances at higher SNR margins are less as compared to smaller hop distances, where more number of hop are required to achieve the same CR. For instance, to achieve a CR of 200, Th-OLA with $\mu = 8$ requires 20% less total energy as compared to Th-OLA with $\mu = 5$ for $\gamma = 14$ and $\psi = 14\text{dB}$. Hence, larger hop distances are more energy efficient at higher SNR margins and also reduces the latency of the networks.

The performance of our proposed thinning algorithm is also compared with the independent thinning algorithm of a PPP and the results are shown in Fig. 13. In independent thinning, random nodes are deleted independently in one level with probability $1 - p$ and the remaining nodes are allowed to transmit with probability p . The process after thinning still follows another PPP with reduced intensity $p\lambda$ and same area, whereas in our proposed algorithm the effective area of the hop reduces keeping the intensity intact. It can be observed that at lower values of CR, our proposed algorithm and the independent thinning process are almost similar but as the values of CR increases, our algorithm outperforms independent thinning. The success probability for independent thinning approach is calculated using μ , as the hop area does not change, whereas for Th-OLA, $\tilde{\mu}$ is used, which effectively reduces the effect of the path loss for the Th-OLA. For instance, to achieve a CR of 100, Th-OLA requires 11.8% less energy than independent thinning. Hence Th-OLA is more energy efficient than independent thinning algorithm for the considered strip-shaped network.

VII. CONCLUSION

We have developed and analyzed a spatial Poisson point process model for a strip-shaped cooperative multi-hop network with random number of nodes and irregular hop boundaries in

the presence of path loss and Rayleigh fading. The Euclidean distance distribution between two randomly located nodes in adjacent levels is derived and approximated with the Weibull distribution for a tractable solution. An analytical expression for the PDF of the received power at a node is derived by self convolving the ratio of an exponential RV and a Weibull RV over a PPP. The received power distribution is used to analyze the network in terms of the one-hop success probability and the m -hop success probability. The analytical model is successful in predicting the coverage range of a pure OLA network under a quality of service constraint. We proposed an energy efficient algorithm based upon the thinning of the total transmitters in one level. It is shown that our algorithm saves a significant amount of energy when compared with basic OLA and it is more efficient than independent thinning. A future direction of this work would be to study the effects of multiple packets transmission in OLA that may induce interference and limit the coverage probability. The effect of shadowing and variable transmit power on the coverage of network is another important direction.

REFERENCES

- [1] J. N. Laneman, D. N. C. Tse, and G. W. Wornell, "Cooperative diversity in wireless networks: Efficient protocols and outage behavior," *IEEE Trans. Inf. Theory*, vol. 50, no. 12, pp. 3062–3080, Dec. 2004.
- [2] J. Lin, H. Jung, Y. J. Chang, J. W. Jung, and M. A. Weitnauer, "On cooperative transmission range extension in multi-hop wireless ad-hoc and sensor networks: A review," *Ad Hoc Netw.*, vol. 29, pp. 117–134, Jun. 2015.
- [3] A. Scaglione and Y.-W. Hong, "Opportunistic large arrays: Cooperative transmission in wireless multihop ad hoc networks to reach far distances," *IEEE Trans. Signal Process.*, vol. 51, no. 8, pp. 2082–2092, Aug. 2003.
- [4] B. Sirkeci-Mersen and A. Scaglione, "A continuum approach to dense wireless networks with cooperation," in *Proc. IEEE INFOCOM*, vol. 4, Mar. 2005, pp. 2755–2763.
- [5] Ç. Çapar, D. Goeckel and D. Towsley, "Broadcast analysis for extended cooperative wireless networks," *IEEE Trans. Inf. Theory*, vol. 59, no. 9, pp. 5805–5810, Sep. 2013.
- [6] S. A. Hassan and M. A. Ingram, "Analysis of an opportunistic large array line network with Bernoulli node deployment," *IET Commun.*, vol. 8, no. 1, pp. 19–26, Jan. 2014.
- [7] A. Afzal and S. A. Hassan, "Stochastic modeling of cooperative multi-hop strip networks with fixed hop boundaries," *IEEE Trans. Wireless Commun.*, vol. 13, no. 8, pp. 4146–4155, Aug. 2014.
- [8] M. Ahsen and S. A. Hassan, "A Poisson point process model for coverage analysis of multi-hop cooperative networks," in *Proc. IEEE Int. Wireless Commun. Mobile Comput. Conf. (IWCMC)*, Aug. 2015, pp. 442–447.
- [9] M. Haenggi and R. K. Ganti, *Interference in Large Wireless Networks*. Boston, MA, USA: Now Publishers Inc., 2009.
- [10] S. A. Hassan and M. A. Ingram, "A quasi-stationary Markov chain model of a cooperative multi-hop linear network," *IEEE Trans. Wireless Commun.*, vol. 10, no. 7, pp. 2306–2315, Jul. 2011.
- [11] Y. Zhang and J. Li, "Wavelet-based vibration sensor data compression technique for civil infrastructure condition monitoring," *J. Comput. Civil Eng.*, vol. 20, no. 6, pp. 390–399, 2006.
- [12] T. L. Willke, P. Tientrakool, and N. F. Maxemchuk, "A survey of inter-vehicle communication protocols and their applications," *IEEE Commun. Surveys Tut.*, vol. 11, no. 2, pp. 3–20, 2nd Quart., 2009.
- [13] M. Haenggi, J. G. Andrews, F. Baccelli, O. Dousse, and M. Franceschetti, "Stochastic geometry and random graphs for the analysis and design of wireless networks," *IEEE J. Sel. Areas Commun.*, vol. 27, no. 7, pp. 1029–1046, Sep. 2009.
- [14] M. Hussain and S. A. Hassan, "Performance of Multi-Hop Cooperative Networks Subject to Timing Synchronization Errors," *IEEE Trans. Commun.*, vol. 63, no. 3, pp. 655–666, Mar. 2015.

- [15] E. S. Sousa and J. A. Silvester, "Optimum transmission ranges in a direct-sequence spread-spectrum multihop packet radio network," *IEEE J. Sel. Areas Commun.*, vol. 8, no. 5, pp. 762–771, Jun. 1990.
- [16] F. J. Massey, Jr., "The Kolmogorov-Smirnov test for goodness of fit," *J. Amer. Statist. Assoc.*, vol. 46, no. 253, pp. 68–78, 1951.
- [17] D. Moltchanov, "Distance distributions in random networks," *Ad Hoc Netw.*, vol. 10, no. 6, pp. 1146–1166, Aug. 2012.
- [18] M. Ahsen and S. A. Hassan, "On the ratio of exponential and generalized gamma random variables with applications to ad hoc SISO networks," in *Proc. IEEE Veh. Technol. Conf. (VTC)*, Sep. 2016, pp. 1–5.
- [19] A. Kostin, "Probability distribution of distance between pairs of nearest stations in wireless network," *IET Electron. Lett.*, vol. 46, no. 18, pp. 1299–1300, Sep. 2010.
- [20] M. K. Simon, *Probability Distributions Involving Gaussian Random Variables: A Handbook for Engineers and Scientists*. USA: Springer, 2007.
- [21] A. Afzal and S. A. Hassan, "A stochastic geometry approach for outage analysis of ad hoc SISO networks in Rayleigh fading," in *Proc. IEEE Global Commun. Conf. (Globecom)*, Dec. 2013, pp. 336–341.
- [22] W. Press et al., *Numerical Recipes in C*, Cambridge, U.K.: Cambridge Univ. Press, 1992.



SYED ALI HASSAN (S'07–M'12) received the B.E. degree (Hons.) in electrical engineering from the National University of Sciences and Technology, Pakistan, in 2004, the M.S. degree in electrical engineering from the University of Stuttgart, Germany, in 2007, and the M.S. degree in mathematics and the Ph.D. degree in electrical engineering from the Georgia Institute of Technology, Atlanta, GA, USA, in 2011. He was a Research Associate with Cisco Systems Inc., CA, USA. He is currently an Assistant Professor with the School of Electrical Engineering and Computer Science (SECS), NUST, where he is the Director of the Information Processing and Transmission Research Group, with a focus on various aspects of theoretical communications. He has co-authored over 75 publications in international conferences and journals. His broader area of research is signal processing for communications. He served as a TPC Member of the IEEE WCSP 2014, the IEEE PIMRC 2013–2014, the IEEE VTC 2013, and the MILCOM 2014–2016.



MUHAMMAD AHSEN received the B.E. degree in electrical engineering from the National University of Sciences and Technology (NUST), Islamabad, Pakistan, in 2013, and the M.S. degree (Hons.) in electrical engineering from the School of Electrical Engineering and Computer Science (SECS), NUST, in 2016. During his M.S., he was a Lab Engineer and a Teaching Assistant with SECS, NUST. He was also a Graduate Researcher with the Information Processing and Transmission Laboratory, SECS, NUST. His research interest mainly lies in wireless communication, cooperative communications, wireless networks, and signal processing. During his M.S., he received the most prestigious President Gold Medal.



DUSHANTHA NALIN K. JAYAKODY (M'12) received the B.E. degree (Hons.) in electronics engineering from Pakistan in 2009 and was ranked as the merit position holder of the University (under SAARC Scholarship), the M.Sc. degree (Hons.) in electronics and communications engineering from the Department of Electrical and Electronics Engineering, Eastern Mediterranean University, Turkey, in 2010, (under the University full graduate scholarship) and ranked as the first merit position holder of the Department, and the Ph.D. degree in electronics, electrical and communications engineering from the University College Dublin, Ireland, in 2014. Since 2014, he has held a Post-doctoral position with the Coding and Information Transmission Group, University of Tartu, Estonia and University of Bergen, Norway. He is currently a Professor with the Department of Software Engineering, Institute of Cybernetics, National Research Tomsk Polytechnic University, Russia. He has served as a Session Chair or a Technical Program Committee Member for various international conferences, such as the IEEE PIMRC 2013/2014, the IEEE WCNC 2014/2016, and the IEEE VTC 2015.

• • •